Batteries & Supercaps

Review
doi.org/10.1002/batt.202400680

Chemistry Europe
European Chemical Societies Publishing

www.batteries-supercaps.org

Alternative Multivalent Metal Elements for Aqueous Hybrid Supercapacitors

Yan Huang,[a, b] Guang Yu,[a, b] Yujia Cheng,*[a, b] Ni Wang,[a] and Wencheng Hu*[a]

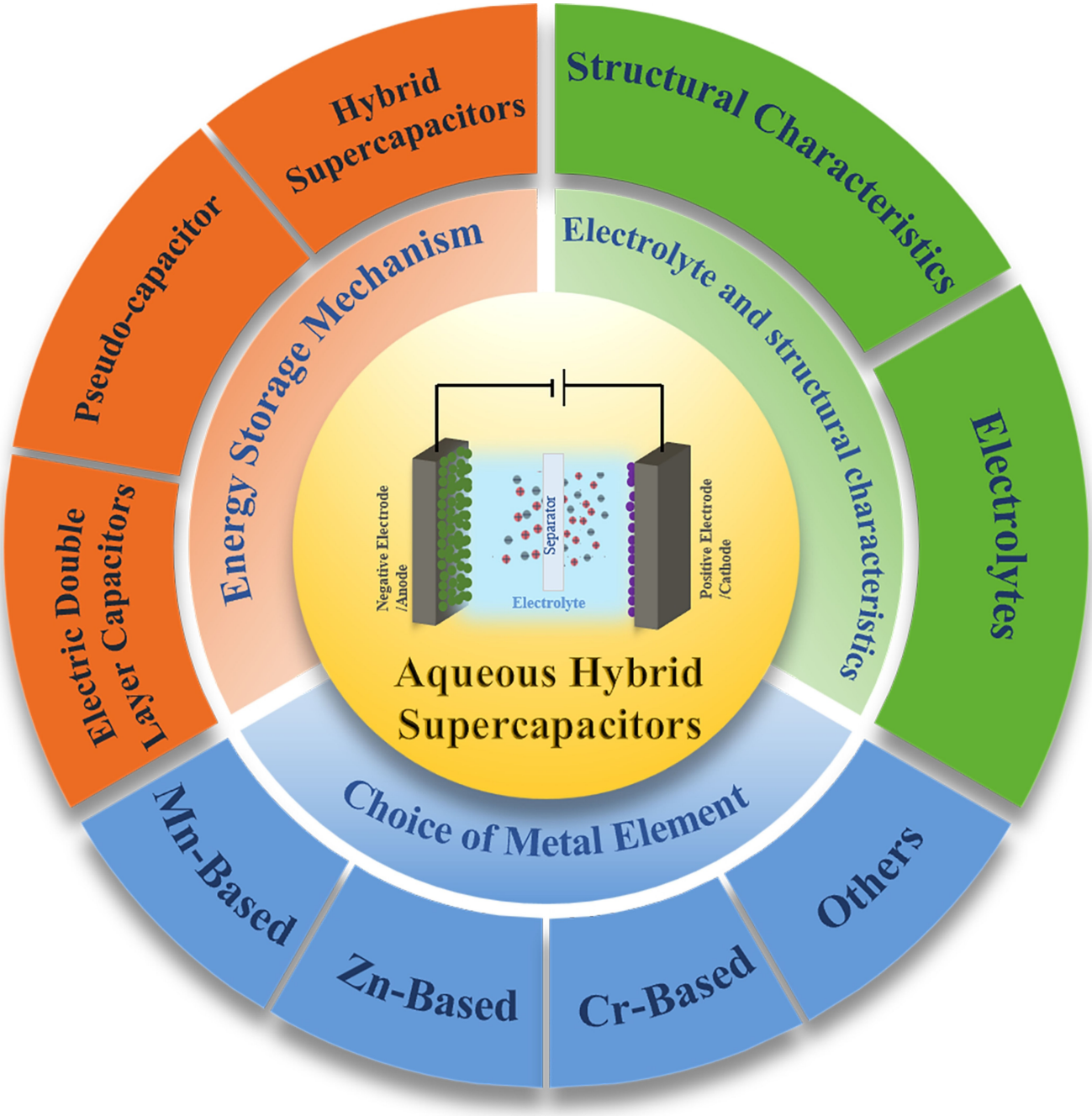

Review
doi.org/10.1002/batt.202400680

Chemistry Europe
European Chemical Societies Publishing

The growing importance of sustainable and clean energy sources is a direct consequence of the increasing scarcity of non-renewable resources and the necessity for energy storage solutions that are safe, efficient, and adaptable. Aqueous hybrid supercapacitors (AHSCs) have garnered attention due to their advantageous characteristics, including low cost, safety, reliability, and high cyclic stability. Here, this review provides a brief overview of the energy storage mechanisms of double electric layer capacitors (EDLCs), pseudocapacitors, and hybrid supercapacitors (HSCs), which combine the features of both of these types of capacitors. The progress made in recent years in research on AHSCs using multivalent metal cations, including manganese, zinc, and chromium, is highlighted. Additionally, some examples of AHSCs assembled with the participation of metal ions are summarized based on the metal activity series. Furthermore, the potential use of other multivalent metals, including iron, cobalt, nickel, and copper, in AHSCs electrodes was explored, as well as the current status of aqueous ammonium-ionized HSCs, with a focus on their respective advantages and challenges. Finally, this review proposes future research directions to further advance this field.

1. Introduction

The global economy is undergoing rapid development, which is resulting in an increased demand for energy resources. This is particularly salient in the context of the diminishing availability of non-renewable resources, which has led to a pronounced emphasis on the exploration of alternative energy sources. These resources encompass coal, oil, and natural gas. The objective is to identify sustainable, secure and clean energy. This objective aligns with the goals of sustainable development.[1,2] However, the direct utilization of renewable energy often requires alignment with specific application scenarios. Consequently, the development of energy storage devices for the conversion of renewable resources has garnered significant attention.[3–5]

Among the various energy storage technologies, electrochemical energy storage devices are distinguished by their repeatable charging and discharging capabilities, high efficiency, and adaptability to diverse application scenarios. These characteristics position them as a promising technological direction for addressing energy storage challenges.[6] To broaden the application scenarios of these energy storage devices, it is essential that they meet the requirements of high energy density, high power density, and durability, while also considering factors such as safety, portability, and cost-effectiveness.[7] Currently, the primary electrochemical energy storage devices under investigation are batteries (such as lithium-ion batteries,[8] sodium-ion batteries,[9] zinc-ion batteries,[10] and fuel cells[11]) and supercapacitors (SCs). These devices have demonstrated significant potential for both civilian and military applications.[12] Among these, lithium-ion batteries are one of the most classical electrochemical devices, widely used in smart devices and electric vehicles.[13–15] The charging and discharging process of a lithium-ion battery is depicted in Figure 1a. However, the commercialization of lithium-ion batteries is encumbered by several challenges, including high manufacturing costs, low power density and poor cycling stability. In contrast, SCs, as a novel type of electrochemical energy storage device with the capacity for rapid energy conversion, offer a number of advantages over traditional batteries.[16] These advantages include higher power density, rapid charging and discharging capabilities, a wider operational temperature range, long cycling stability, and the ability to deliver instantaneous high-power charging and discharging. These attributes make SCs a compelling alternative for various energy storage applications.

The two most critical parameters for evaluating the effectiveness of an energy storage/conversion device are energy density and power density. The relationship between these two parameters is illustrated in Figure 1b, which depicts the Ragone plots of various energy storage devices to illustrate the trend of their energy density and power density.[17] As depicted in the figure, batteries exhibit high energy density but relatively low power density. In contrast, electric double-layer capacitors (EDLCs) possess high power density but offer limited advantages in terms of energy density. It is therefore necessary to develop energy storage devices that maintain both high energy density and high-power density. The construction of hybrid supercapacitors (HSCs) presents a promising avenue for addressing this challenge. In previous research, alkaline ion energy storage systems, such as lithium-ion and sodium-ion capacitors, have attracted considerable attention within the scientific community.[18,19] However, these systems are not without their drawbacks. Specifically, the organic electrolytes

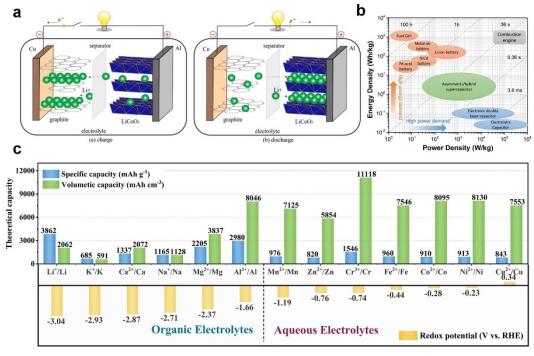

Figure 1. a) Schematic diagram of lithium-ion battery charging and discharging;[8] b) Ragone plots comparing specific power and specific energy of different energy storage devices;[17] c) The theoretical capacities and redox potentials of different metal anodes.[27]

[a] *Y. Huang, G. Yu, Y. Cheng, N. Wang, W. Hu*
School of Materials and Energy, University of Electronic Science & Technology of China, Chengdu 611731, P. R. China
E-mail: chengyujia@zsc.edu.cn
huwc@uestc.edu.cn

[b] *Y. Huang, G. Yu, Y. Cheng*
Zhongshan Institute, University of Electronic Science & Technology of China, Zhongshan 528402, P. R. China

employed in these devices are prone to flammability and exhibit toxicity, which presents considerable safety concerns. Furthermore, the overactive reactions of alkali metals with water or air exacerbate these risks.[20] In contrast, aqueous hybrid supercapacitors (AHSCs) use low-cost, safe and reliable aqueous electrolytes, which are safer and more environmentally friendly than the organic electrolytes employed in commercial lithium-ion batteries. Additionally, these electrolytes do not release toxic substances during charging and discharging, and they possess power densities that meet the power density requirements of SCs.[21–23] In addition, multivalent metal cations show greater potential than alkali metal ions for high-security HSCs applications due to their extensive availability on earth and high capacity to enable multiple electron transfer in electrode reactions.[24] In particular, transition metals corresponding to multivalent cations, such as zinc (Zn), are not only abundant but also exhibit safe and efficient charge storage performance in aqueous solution based on a deposition/dissolution mechanism for battery-type anodes. In addition to Zn, other transition metals corresponding to multivalent cations, including manganese (Mn) and chromium (Cr) have also received extensive attention in the study of AHSCs.[25–28] Figure 1c illustrates the theoretical capacities and redox potentials of certain transition metals as battery anodes, demonstrating the significant impact of the nature of different metal anodes on the structural design of HSCs and the overall performance of the device.[21] While there has been a proliferation of literature reviewing the structural design and prospects of aqueous zinc-ion SCs, a systematic introduction of AHSCs incorporating other transition metal elements is absent.[16,21,29] In this review, the structural features of AHSCs are examined, along with the classification of electrolytes and the selection of multivalent metal elements in AHSCs (Figure 2). This discussion focuses on the advancements in the field of Mn-, Zn-, and Cr-based AHSCs, as well as the applications of Fe-, Co-, Ni-, and Cu-based materials in AHSCs are also introduced. Furthermore, the current challenges and future research directions of the multivalent metals in AHSCs are also discussed.

2. Energy Storage Mechanism of Supercapacitors

2.1. Electric Double Layer Capacitors

SCs can be categorized into EDLCs, pseudocapacitors, and hybrid capacitors based on their energy storage mechanisms

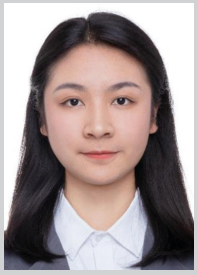

Yan Huang is currently pursuing a Master's Degree in Applied Chemistry at the University of Electronic Science and Technology of China. She holds a Bachelor's Degree in Applied Chemistry from Xihua University, with a strong foundation in Electrochemistry. Her research interests primarily focus on the nanostructure materials for supercapacitors.

Guang Yu is an Assistant Professor at the Zhongshan College, University of Electronic Science and Technology, Zhongshan, China. He holds a PhD from Harbin University of Science and Technology and worked as a Postdoctoral Fellow at the University of Electronic Science and Technology, specializing in composite nanomaterials for electron devices. His research interests include the development of nanomaterials with novel structures for electrochemistry and the application of these materials in the construction of energy storage devices.

Associate Professor Yujia Cheng, Ph.D., is currently working in the School of Electrical and Mechanical Engineering, Zhongshan College, University of Electronic Science and Technology, as an associate professor of electrical engineering. She specializes in the synthesis, preparation, structural characterization, and dielectric properties of polymer-based nanocomposite insulating materials, and has participated in a number of National Natural Science Foundation of China projects.

Ni Wang is a Professor of the School of Materials and Energy at the University of Electronic Science and Technology, located in Chengdu, China. She received her BS and MS in Applied Chemistry PhD in Materials Science and Engineering from the University of Electronic Science and Technology in 2009, 2011, and 2017, respectively. She has authored and co-authored more than 50 research papers in the area of energy storage materials and devices. Since 2022, she has been a leader scientist at the Nanocomposites and Applied Electrochemistry Group, specializing in nanomaterials for novel energy storage devices.

Prof. Wencheng Hu received his B.S., M.S., and PhD degrees from the Chengdu Institute of Radio Engineering, the Chengdu University of Science and Technology, and the University of Electronic Science and Technology of China. Since 2007, he has been a professor at the University of Electronic Science and Technology of China. His current research focuses on applied electrochemistry.

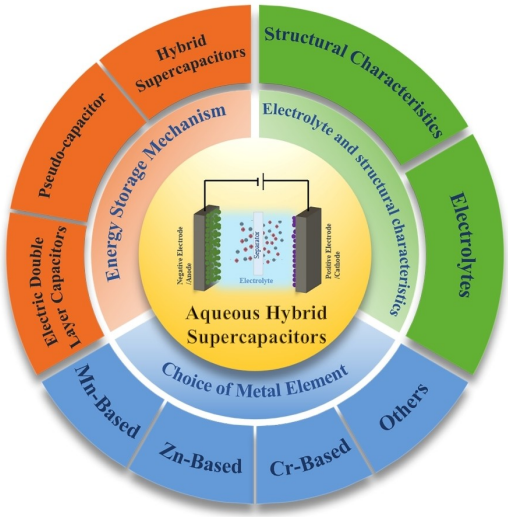

Figure 2. Schematic illustration showing the classification of SCs and their energy storage mechanisms, structural features of AHSCs and selection of multivalent metal elements in AHSCs Schematic illustration showing thein this review.

and the types of electrode materials used.[30] In EDLCs, charge storage does not involve charge transfer but relies on electrostatic interactions between charge ions and the electrodes (Figure 3a). An external electric field induces the migration of anions and cations in the electrolyte to the respective electrodes. When charge accumulation occurs on the electrode surfaces, ions with opposite charges in the nearby electrolyte migrate to the electrodes and accumulate on their surfaces, forming a double electric layer between the electrodes and the electrolyte.[31] This charge accumulation is a non-Faradaic process.[32] During charging, electrons move from the positive to the negative electrode in an external circuit, and the anions and cations in the electrolyte move towards the positive and negative electrodes, respectively. During the discharging process, the movement of ions is reversed.[33,34] This process does not involve significant redox reactions and is characterized by rapid ion adsorption and desorption.[35] It is therefore highly reversible and usually exhibits complete reversibility. As a result, the electrochemical behavior of EDLCs is specific to the CV and GCD curves. Its CV curve usually shows a rectangular symmetric shape with no obvious redox peaks, which indicates that the charge storage mainly depends on the charge separation at the electrode-electrolyte interface. In contrast, on the GCD curve, EDLCs show a linear or nearly linear relationship, with the voltage decreasing in a straight line over time. This indicates that the charging and discharging processes are almost completely reversible, reflecting their highly efficient energy storage and release characteristics. The most extensively researched and utilized electrode materials for EDLCs encompass a range of carbon-based substances, including activated carbon (AC),[36,37] graphene or reduced graphene oxide (rGO),[38,39] carbon nanotubes (CNTs),[40] and carbon aerogels (CA).[41,42]

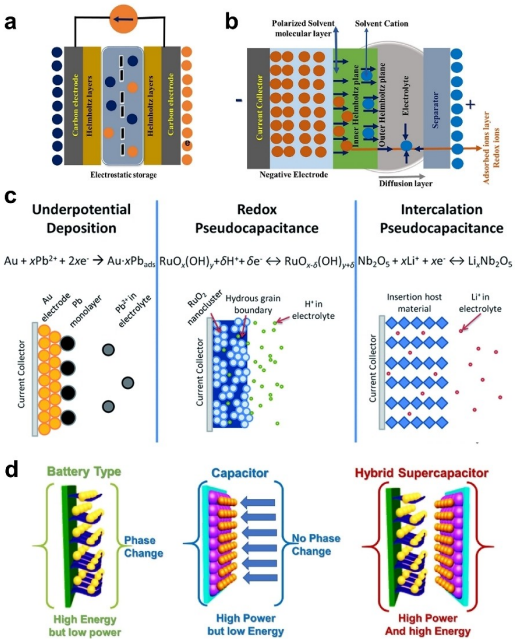

Figure 3. a) Schematic presentation of electrical double-layer capacitor;[58] b) Schematic presentation of pseudocapacitors;[58] c) Different types of reversible redox mechanisms that give rise to pseudocapacitance: underpotential deposition, redox pseudocapacitance, and intercalation pseudocapacitance;[44] d) Schematic presentation of charge storage mechanism of HSCs.[58]

2.2. Pseudocapacitors

Pseudocapacitors store charge primarily through rapid and highly reversible redox reactions at the electrodes(Figure 3b).[43] In contradistinction, the electrochemical characteristics of pseudocapacitors deviate from those of EDLCs.[35] The CV curves show obvious redox peaks, which denote the redox reactions occurring in the active substances present within the electrode materials.The GCD curve may exhibit nonlinear characteristics, particularly the voltage drops rapidly at the commencement of the discharge and subsequently stabilises. Furthermore, the GCD curves may exhibit a certain hysteresis phenomenon, indicating the presence of more complex electrochemical reactions in the charging and discharging processes. The superior energy storage performance of pseudocapacitors, in comparison to EDLCs, is largely attributed to the facilitation of electron transfer processes, including charge transfer and ion intercalation. As delineated in Figure 3c, pseudocapacitors can be differentiated into three principal categories based on their underlying charge storage mechanisms: underpotential deposition pseudocapacitors, surface redox pseudocapacitors, and intercalation pseudocapacitors.[44] Underpotential deposition is characterized by a deposition process wherein a solid phase substance with a low work function is deposited onto a high work function metal surface at potentials that exceed the theoretical reduction potential. A quintessential example of this process is the reduction-mediated deposition of Pb^{2+} on the surfaces of high-cost metals such as Ag, Pt, and Au. However, this mechanism is seldom utilized for energy storage applica-

tions due to the economic impracticality associated with the use of such costly metal substrates.[45] The surface redox and intercalation pseudocapacitance mechanisms are particularly emblematic of the energy storage processes within pseudocapacitor SCs. The mechanism of surface redox pseudocapacitance is characterized by the deposition of charges on the surface of the electrode material through a series of sustained and reversible redox reactions.[46] The materials most commonly employed in this mechanism are predominantly transition metal oxides, such as RuO_2 and MnO_2, as well as conductive polymers including polyaniline and polypyrrole.[47,48] Intercalation pseudocapacitance involves charge storage not only at the surface but also within the crystalline lattice of materials that possess one-dimensional or two-dimensional channels.[49] Because of the limited degree of solid-state phase transition during the reaction and the accompanying minimal lattice strain, the embedded pseudocapacitor is capable of rapidly storing charges over a brief period. Notable examples of materials that demonstrate this behavior include MoS_2, TiS_2, and transition metal carbides (MXene).[50–52]

Pseudocapacitor behavior involves not only redox reaction processes but also the potential for diffusion into the bulk phase of the material. Consequently, pseudocapacitors tend to have greater capacity than double-layer capacitors. However, the embedding and de-embedding processes of ions during the redox process can have adverse effects on the structure of the electrode material, such as volume changes, which can lead to the possible collapse of the structure, and therefore pseudocapacitors tend to have less cycling stability than double layer capacitors, yet they demonstrate a longer cycling life than batteries.[53] Currently, the main pseudocapacitor electrode materials include conducting polymers, transition metal oxides, transition metal sulfides, and transition metal hydroxide materials.

2.3. Hybrid Supercapacitors

In general, HSCs combine the properties of the first two, with the presence of two distinct charge storage mechanisms: a double-layer capacitive type and a battery-type redox type (Figure 3d). The concept of hybrid energy storage devices was first introduced in 2001 by Amatucci's team,[54] who employed activated carbon as the capacitive positive electrode and nano $Li_4Ti_5O_{12}$ as the battery-type negative electrode to create a hybrid energy storage device. This device demonstrated a capacity utilization rate of 90% at a charge/discharge rate of 10 C, accompanied by a capacity loss of 10% to 15% after 5000 cycles, and an energy density of up to 20 $kW\,kg^{-1}$. The architecture of these hybrid systems is predicated on the synergistic interaction between double-layer capacitor electrodes and pseudocapacitor electrodes, which collectively contribute to electrochemical energy storage.[55] This configuration not only results in a supercapacitor with enhanced chemical stability but also confers a higher energy density relative to conventional single-nature capacitors.[56] Additionally, these devices exhibit superior power density and cycling stability compared to traditional batteries.[57] The strategic integration of these properties effectively bridges the performance gap delineated by the Ragone plot between EDLCs and batteries and fulfills the new type of needs of energy storage devices.

3. Classification of Electrolytes and Structural Characteristics of Water-Mixed Supercapacitors

3.1. Classification and Characterization of Electrolytes

Electrolyte plays a crucial role in electrochemical supercapacitors, serving not only as an ionic conductor and electronic insulator that facilitates connectivity between disparate electrodes, but also being regarded as the "blood" of electrochemical energy storage devices. The efficacy of electrolytes exerts a direct influence on the operational temperature range, safety performance, multiplication performance, cycle efficiency, and storage performance of supercapacitors. Consequently, when selecting an electrolyte, it is imperative to take into account the type and concentration of the electrolyte, the size of the anion and cation, the type of solvent, and the interaction between the electrolyte and the electrode.[59] The ideal electrolyte should be characterized by a wide electrochemical window, high ionic conductivity, low viscosity, wide operating temperature range, good stability, environmental friendliness, low cost and safety.[60] Currently, electrolytes are mainly categorized into aqueous electrolytes, organic electrolytes and ionic liquid electrolytes.[61]

Organic electrolytes, consisting of organic solvents and conductive salts, are widely used in commercial EDLCs due to their capacity to offer a broad voltage window of 2.5 V~3.5 V,[62] which effectively safeguards the energy storage capability of electrochemical energy storage devices. Typical organic electrolytes consist of organic solvents such as acetonitrile (ACN) or propylene carbonate (PC), and conductive salts such as tetraethylammonium tetrafluoroborate ([TEA][BF_4]) and triethyl methylammonium tetrafluoroborate ([TEMA][BF_4]). However, these organic solvents are highly flammable and volatile, leading to serious safety and environmental issues for energy storage devices, especially in large-scale applications such as rail transportation and power systems. In addition, the toxicity of organic solvents poses a threat to the environment and human life.

Ionic liquids, which consist of a large volume of asymmetric organic cations coupled with inorganic or organic anions, are liquid at or near room temperature and have extremely low volatility and vapor pressure,[63] as well as high chemical stability and good thermal stability. These properties have led to the widespread interest in ionic liquids in electrochemical research, especially for applications in supercapacitors, where they exhibit a remarkable electrochemical stability window extending up to approximately 4.5 V.Ionic liquids possess a high degree of structural diversity, which can be systematically tailored to modulate their properties, making them suitable for a wide range of applications. Notable examples of commonly

used ionic liquids in supercapacitors include pyrrolidine, imidazole, and aliphatic quaternary ammonium salts in combination with anions such as PF_6^-, BF_4^-, $TFSI^-$, and FSI^-. However, it should be noted that ionic liquids are expensive, highly viscous, and strongly hygroscopic, factors that have a detrimental effect on key device properties such as power density, operating voltage window, and cycling stability.[64,65]

Aqueous electrolytes can be categorized as acidic, neutral or alkaline based on their pH. Water is the most abundant solvent on Earth, consequently, its production costs are significantly lower than those of ionic liquids or organic solvents that rely on petroleum products. The non-flammable and non-toxic nature of aqueous electrolytes gives them excellent safety and environmental friendliness. Water's high dielectric constant, large dipole moment, and excellent acceptor and donor capabilities make it a highly efficient solvent for salts, ensuring that aqueous electrolytes have superior ionic conductivity, which is often far superior to organic electrolytes and ionic liquids.[66] In comparison, aqueous electrolytes exhibit significant advantages in terms of safety, ionic conductivity, environmental compatibility, ease of operation and cost-effectiveness. Consequently, it is regarded as a promising substitute for conventional organic electrolytes and plays a pivotal role in the development of eco-friendly and sustainable energy storage devices.[67]

3.2. Structural Characteristics of Aqueous Hybrid Supercapacitors

AHSCs have emerged as a prevalent subject of contemporary research in the domain of energy storage. It is distinguished by several advantageous characteristics, including low cost, safety, reliability, environmental benignity, superior cycling stability, and rapid kinetic response characteristics. Typically, AHSCs are constructed in an asymmetric format, integrating capacitor-type and battery-type electrodes to synergize the distinct advantages of two energy storage paradigms, thereby enhancing the overall performance of the device.[68,69]

During the charge and discharge cycles, the AHSCs facilitate rapid energy transfer through the accelerated adsorption/desorption of ions on the electrode surface and the reversible dissolution/deposition processes.[70] Capacitive electrodes composed of materials endowed with a high specific surface area, provide a multitude of active sites that catalyze rapid ion dynamics. Upon charging, electrolyte ions, exemplified by hydrogen ions, are drawn to the electrode surface by the electric field, establishing a double electric layer and effectuating the physical storage of energy devoid of chemical transformations within the electrode material. Conversely, during discharge, these ions are liberated into the electrolyte and migrate towards the counter electrode, thereby releasing energy for utilization by the external circuit. The physical nature of this adsorption and desorption mechanism endows the capacitor with the capability for rapid charge and discharge within a period of seconds to minutes. In contradistinction to the capacitive energy storage mechanism, the battery-type energy storage within the AHSCs involves a chemical alteration of the electrode material. Battery-type electrodes partake in oxidation reactions during charging, liberating cations into the electrolyte. For instance, the oxidation of a zinc electrode is depicted by the reaction $Zn \rightarrow Zn^{2+} + 2e^-$. During discharge, these ions are reduced and deposited on the electrode surface, reinstating the material to its pristine state, as exemplified by the reduction reaction $Zn^{2+} + 2e^- \rightarrow Zn$. This dissolution/deposition process is characterized by reversibility, ensuring the capacitor's performance is sustained across numerous charge/discharge cycles.

The hybrid configuration of the AHSCs has the effect of broadening the operational voltage window and augmenting the energy density. Furthermore, it amalgamates the swift charge/discharge attributes of the capacitor-based electrodes with the chemical robustness of the battery-based electrodes, thereby achieving a balance between rapid response and cycling stability. Through the optimization of electrode materials and the electrolyte, the AHSCs are capable of sustaining stable performance over an extended duration of charge/discharge cycles, thereby reducing capacity degradation and enhancing the longevity of the device.

4. Aqueous Hybrid Supercapacitors

4.1. Manganese-Based Hybrid Supercapacitors

In the development of pseudocapacitors and battery-type electrodes, it is essential to consider the redox properties of the materials utilized. Transition metal elements with multiple valence states offer a wide range of options for selection, which is a crucial factor in the optimization of these devices. Excellent electrode materials frequently exhibit reversible redox reactions, structural stability, low cost, environmental friendliness, and a relatively low molar mass. Mn, a transition metal with the third-highest crustal abundance and abundant natural reserves, offers the potential for reduced manufacturing costs. Furthermore, Mn has five unpaired electrons in its outermost electron shell, leading to a variety of valence states. The distinctive electronic structure of Mn makes it highly redox-active, thereby rendering Mn-based electrode materials widely applicable in energy storage devices.

Manganese-based electrode materials, particularly manganese oxide and manganese sulfide, are common forms of SCs. These materials can be synthesized through a variety of methods, including hydrothermal synthesis,[71,72] precipitation,[73,74] and chemical vapor deposition (CVD).[75,76] Notably, manganese dioxide (MnO_2) has garnered significant attention as an electrode material for SCs, which is attributed to its non-toxic nature and its substantial theoretical specific capacitance (~1370 $F g^{-1}$).[77] In order to enhance the electrochemical performance of MnO_2, various strategies have been employed, including morphological engineering, defect engineering, and heterojunction engineering. In recent years, morphological engineering, defect engineering and heterojunction engineering have been employed to modify MnO_2 to

enhance its electrochemical properties. Emin et al., for instance, prepared a hierarchical electrode structure of Ni–Mn layered double hydroxide (Ni–Mn–LDH) loaded MnO_2 on nickel foam using electrodeposition and hydrothermal synthesis.[78] The SEM image of this electrode is shown in Figure 4a. The AHSC combined with the activated carbon anode demonstrated an energy density of 104.51 W h kg^{-1} at 800.00 W kg^{-1} in a 3 M KOH electrolyzed aqueous solution, which represents a superior performance compared to the previously reported value (Figure 4b). Moreover, the composite exhibited noteworthy cycling stability, with 86.8% retention of its initial capacitance after 22000 consecutive charge/discharge cycles, as illustrated in Figure 4c. The combination of LDHs and TMOs in a heterostructure composite electrode material offers a solution to the low specific capacitance of LDHs, whilst also enhancing the multiplicity and cycling stability of TMOs. This combination utilizes the exposed layered active materials to their full potential, generating synergistic effects that optimize ion intercalation, chemical/physical adsorption, and chemical reactions, thus resulting in improved specific capacitance. Subsequently, Zhang et al. developed a CNF/CNT/ MnO_2 composite electrode through the technique of electrochemical deposition.[79] Furthermore, Li et al. reported the preparation of a GO/MnO_2/CoNi-LDH composite electrodeposited onto an activated carbon cloth (CC/GMCN) using a sequential deposition methodology.[80] The introduction of GO brings excellent conductivity and abundant active sites to the electrode materials. The incorporation of MnO_2 serves to broaden the voltage window of the electrode materials, thereby enhancing the overall specific capacitance through its augmented voltage window and heightened theoretical specific capacitance. Concurrently, the amalgamation of CoNi–LDH with MnO2 and GO further augments the overall specific capacitance and cycling stability of the electrode materials by virtue of its enhanced specific capacitance and favorable cycling stability. The assembled AHSC, with activated carbon serving as the negative electrode, delivered an energy density of 82.12 Wh kg^{-1} at a power density of 949.97 W kg^{-1}(Figure 4d). Figure 4e shows that the device maintains 92.62% capacity retention after 10,000 charge/discharge cycles. This is attributed to the significant role played by the heterogeneous interfaces between the three materials, which facilitate charge transfer and ion diffusion, thereby enhancing the electrochemical performance of the electrode materials.

The metal Mn is the final metal in the order of activity table of the metals table that can be deposited directly from an aqueous solution, which is because H_2 has a large overpotential on the metal Mn. Consequently, during the electrolytic process, the Mn^{2+} ions in the aqueous electrolyte are reduced and deposited onto the cathode, thereby forming metallic Mn monomers. Furthermore, the formation of the MnO_2 electrode material is achieved through the oxidation of Mn^{2+} and subsequent deposition on the anode. This direct deposition method represents an economical and efficient approach to fabricating MnO_2 electrode material on current collectors, which has garnered widespread adoption in the field.[81] Currently, there is a burgeoning interest in the development of Mn^{2+} -based all-manganese energy storage devices (AMnESDs). For instance, Hu's team devised a one-step co-deposition method for assembling AMnESDs using a porous carbon cloth (NPCF) and a hybrid electrolyte comprising $MnSO_4$ and $(NH_4)_2SO_4$ hybrid electrolyte, based on the redox chemistry of Mn^{2+}.[26] The SEM image of the reduced product deposited on the surface of NPCF (Figure 5a) illustrates that the negative product is observed to be uniformly attached to the surface of NPCF, which can be attributed to the effective deposition of metal Mn particles on the surface of NPCF. Figure 5b shows the SEM image of the oxidized product deposited on the surface of NPCF, and the attached particles on the surface of NPCF are observed to be substituted, which is due to the uniform deposition of manganese oxides on the surface of NPCF. The XRD patterns in Figure 5c provide accurate evidence for the generation of α-Mn and Mn_3O_4; the diffraction peaks observed by XRD in Figure 5d are all in good agreement with ε-MnO_2. The cycling performance of AMnESD was tested at a high current density of 15 mA cm^{-2} (Figure 5i), demonstrating a capacity retention of nearly 93.5% after 40000 cycles. In

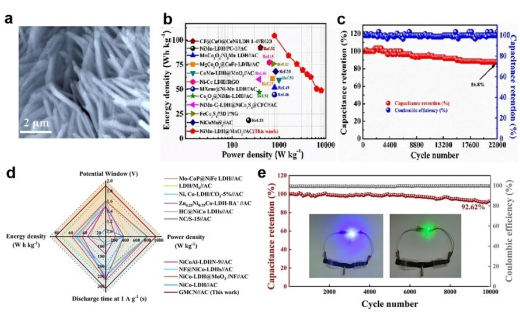

Figure 4. a) SEM images of NiMn-LDH@MnO_2;[78] b) Comparison of Ragone plots with the published values;[78] c) Cycling performance and Columbic efficiency during 22000 cycles at 5 A g^{-1};[78] d) Comparison of energy density, power density, voltage window and discharge time at 1 A g^{-1} of GMCN//AC obtained in this work with previous work;[80] e) Capacitance retention and coulombic efficiency of GMCN//AC at 5 A g^{-1} for 10,000 cycles, insets of the optical pictures of two devices connected in series lighting a 3 V blue LED and a 3 V green LED.[80]

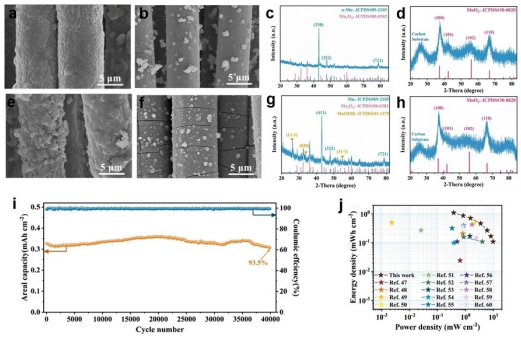

Figure 5. a) FESEM images of reduction product on NPCFC in 3 M $MnSO_4$ + 0.5 M $(NH_4)_2SO_4$ plating solutions;[26] b) FESEM images of MnO_2 cathode;[26] c) XRD pattern of Mn anode;[26] d) XRD pattern of MnO_2 cathode;[26] e) Characterization results of Mn cathode after 40000 cycle test;[26] f) Characterization results of MnO_2 cathode after 40000 cycle test;[26] g) XRD pattern of Mn anode; h) XRD pattern of MnO_2 cathode;[26] i) The cycle performance at 15 mA cm^{-2},[26] j) the Ragone plot.[26]

addition, Hu's group performed SEM analysis of the positive and negative electrode materials after cycling (Figure 5e avd f). They observed that the thickness of the autoxidized layer of metallic Mn gradually increased on the negative electrode as the reaction progressed; whereas, the morphology of the MnO_2 positive electrode did not undergo any significant change, and the nanoparticles were firmly encapsulated on the surface of the NPCF (compared to Figure 5a avd b). The XRD patterns of the negative electrode after the cycling test in Figure 5g confirm the persistence of the α-Mn phase, in addition to the presence of the Mn_3O_4 and MnOOH phases. The latter may be attributed to the precipitation of hydrogen. The reaction occurring on the electrode surface during the cycling test is also confirmed by the XRD analyses in Figure 5h, which show that the composition of the cathode material's physical phase has not changed and that it is still MnO_2 with a low degree of crystallinity. These results provide definitive confirmation that the assembled AMnESD exhibits unparalleled cycling stability. Furthermore, the AMnESD devices assembled using PGCF bases demonstrated an energy density of up to 1.14 mWh cm^{-2} and a maximum power density of 9.70 mW cm^{-2} (Figure 5j). By optimizing the electrolyte, employing a high-performance collector material, NPCF, and improving the electrochemical conversion mechanism, Hu's team significantly enhanced the electrochemical performance of AMnESDs, including cell capacity, multiplicity performance, and cycling stability. The results of this research provide new ideas for the design of low-cost, high-energy, and high-stability aqueous batteries, and demonstrate the excellent performance of these devices in terms of charge storage performance and cycling stability, which provides valuable insights for the development of cost-effective, high-energy, and high-stability manganese-based AHSCs.

4.2. Zinc-Based Hybrid Supercapacitors

The development of metal-ion HSCs with reduced cost and enhanced safety for applications necessitates rigorous safety standards, and thus ZHSCs are gradually gaining prominence. Metal Zn possesses a high theoretical volumetric capacity of 5854 mAh cm^{-3} and a high theoretical mass capacity of 820 mAh g^{-1}. Furthermore, the oxidation/reduction potential is as low as −0.76 V compared to standard hydrogen electrodes, which suggests that a high open-circuit voltage may be present when it is combined with the cathode. Consequently, ZHSCs have garnered significant interest within the field of energy storage devices.[82–84]

The extant literature on ZHSCs has predominantly concentrated on the advancement of high-capacity carbon-based positive electrodes for device construction, with metallic zinc sheets employed as negative electrodes. For instance, Li et al. fabricated a hierarchically structured nanocomposite of hollow carbon nanotubes (h-CNTs) and PANI via an in situ polymerization technique.[85] The SEM image in Figure 6a illustrates the nanocomposite's morphology. The incorporation of PANI not only augmented the cathode's redox reaction energy storage

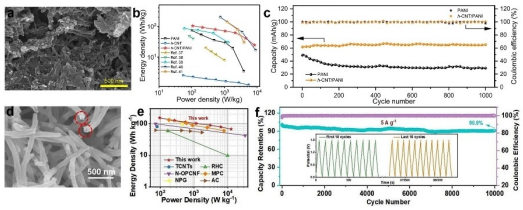

Figure 6. a) SEM images of h-CNT/PANI nanocomposite;[85] Electrochemical performance of pure PANI and h-CNT/PANI nanocomposite cathodes: b) Ragone plots;[85] c) Cycling performance;[85] d) Schematic diagram of PCNTs preparation. SEM images PCNTs-6;[86] e) Ragone plots of Zn//PCNTs-6 compared with some reported ZISCs with activated carbon-based cathodes;[86] f) Cycle performance of Zn//PCNTs-6 at 5 A g^{-1} (inset: the first 10 and the last 10 GCD curves).[86]

capacity but also enhanced its mechanical integrity. The ZHSC assembled with the h-CNT/PANI nanocomposite as the cathode demonstrated superior electrochemical performance, as depicted in Figure 6b. Moreover, the h-CNT/PANI nanocomposite cathode displayed remarkable cycling stability, with a capacity retention of 65 mAh g^{-1} after 1000 charge/discharge cycles at a current density of 1 A g^{-1}, as shown in Figure 6c. Throughout the extended cycling test, the Coulombic efficiency consistently exhibited a consistent approach to 100%. In another study, Huo et al. synthesized porous carbon nanotubes derived from PCNTs through the carbonization and activation process of polypyridine carbon nanotubes, which were templated by oxidation.[86] The SEM image in Figure 6d indicates that the PCNTs preserved the tubular architecture of the polypyridine precursor while acquiring a porous structure and surface functional groups conducive to Zn^{2+} ion intercalation. The resulting zinc-ion HSCs achieved an actual energy density of 10.7 Wh kg^{-1} and an impressive power density of 192.2 W kg^{-1}, surpassing the performance of the majority of previously reported zinc-ion energy storage devices, as illustrated in Figure 6e. Furthermore, the Zn-ion hybrid supercapacitor exhibited remarkable cycling stability, with a capacity retention of 90.9% and a Coulombic efficiency of 99.9% for the Zn//PCNTs-6 configuration after enduring 10000 cycles at a substantial current density of 5 A g^{-1}, as detailed in Figure 6f. These innovative approaches have proven efficacious in augmenting the energy density of carbon-based cathodes, thereby propelling the development of ZHSCs towards higher energy and power densities, and enhancing their cycling stability, which is critical for the advancement of next-generation energy storage technologies.

The incorporation of an excessive amount of metallic zinc into the system can impede the accurate assessment of the device's actual capacity and its overall performance metrics, including cycling stability. Furthermore, during the zinc deposition phase, the occurrence of HER and corrosion at the electrode/electrolyte interface can have a detrimental impact on the reversibility of the metallic zinc deposition/stripping process. Additionally, due to the gradient distribution of Zn^{2+} ions, the local accumulation of space charge, and the non-uniformity of the high-power electric field, the zinc anode is susceptible to preferential metallic deposition in specific crystallographic orientations, leading to the formation of zinc

dendrites. In a recent study by Sun et al., a particular emphasis was placed on achieving uniform deposition of metallic zinc and enhancing the reversibility of the zinc deposition/exfoliation process on carbon fiber surfaces.[25] This was accomplished through a straightforward method of fabricating high-performance ZHSC on PGCF substrates, as depicted in Figure 7a. Figure 7c avd d present the SEM and XRD patterns of the Zn@PGCF anode, respectively. It can be observed that micrometer-scale particles with smooth surfaces have adhered uniformly to the PGCF substrate. In contrast to the dense, lump-like structures where the dissolution and deposition of metallic zinc are confined to the top layer, the electrode structure in question facilitates zinc dissolution at both the top and bottom of the zinc layer, thereby exhibiting superior activity in terms of CE. The Ragone plot in Figure 7e illustrates that the ZHSC-LZC-9H device delivers an energy density of up to 2.02 mWh cm^{-2} at a power density of 0.43 mW cm^{-2} while sustaining an energy output of 0.45 mWh cm^{-2} at an elevated power density of 11.47 mW cm^{-2}. The device, based on two PGCF substrates, has been demonstrated to have superior charge storage capability in comparison to previously reported aqueous ZHSC devices. Moreover, as shown in Figure 7b, the device demonstrates exceptional cycle stability, maintaining consistent performance for 30000 cycles at 20 mA cm^{-2} with an output of 0.75 mAh cm^{-2}. The anode results from the post-cyclic testing, as presented in Figures 7f avd g, indicate that the particle morphology remains intact, with no discernible dendritic structures. The charge-discharge capacity curves at various low temperatures, as shown in Figure 7i, reveal that the ZHSC maintains a stable output capability at constant temperatures, with minimal capacity degradation due to multiple temperature fluctuations. Furthermore, the device recovers to its initial capacity upon direct heating from −60 °C to room temperature, despite the potential degradation of electrochemical conductivity caused by sluggish ionic dynamics and changes in electrolyte viscosity at low temperatures. As demonstrated in Figure 7j, the ZHSC device displays remarkable cycling stability in the context of extreme cold conditions, retaining 90.7% of its capacity after 5000 charging-discharging cycles at 8 mA cm^{-2}. In conjunction with the Ragone plots in Figure 7h, it is evident that this ZHSC device can still provide an energy density of up to 0.868 mWh cm^{-2} at −60 °C, which is a notable improvement over the low-temperature energy storage capabilities of previously reported aqueous energy storage devices. ZHSC is confronted with challenges such as zinc dendrite formation and side reactions, which impose limitations on its performance and longevity. Current research is inadequate in terms of electrode material design, electrolyte optimization, interface modification and side reaction control. To address these issues, future research should focus on smart electrode design, electrolyte innovation, interface engineering, and in situ monitoring and control. Possible breakthrough directions include the preparation of nanostructured electrodes, the development of multifunctional composites, the application of machine learning and artificial intelligence, and the exploration of environmentally friendly materials. These innovations are expected to enhance the performance and reliability of ZHSC, thus promoting its widespread adoption in practical applications. In addition, research continues to develop high-performance cathode materials to improve the energy density and cycle stability of ZHSCs. Concurrently, there is a necessity to direct greater attention toward the optimization of zinc electrodes in forthcoming research, with the objective of more accurately evaluating the actual integrated level of the overall device. This, in turn, will serve to promote the further development and application of ZHSC technology.

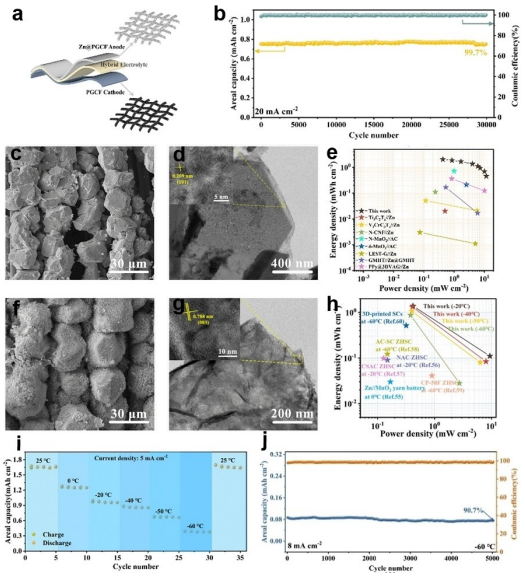

Figure 7. a) The assembly diagram of ZHSC;[25] b) The cycling stability data at 20 mA cm^{-2},[25] c) SEM image of Zn anode before cycling test;[25] d) TEM profile of Zn anode before cycling test;[25] e) Ragone plot at room temperature;[25] f) SEM image of Zn anode after cycling test at 1 mA cm^{-2};[25] g) TEM profile of Zn anode after cycling test at 1 mA cm^{-2};[25] h) Ragone plot at −20 to −60 °C;[25] i) Charge/discharge capacity change from 25 to −60 °C;[25] j) Cyclic stability at −60 °C.[25]

4.3. Chromium-Based Hybrid Supercapacitors

To meet the distinctive requirements of energy storage systems across a range of application contexts, researchers have initiated the design of alternative HSCs with exemplary electrochemical characteristics. In the reactivity series of metals, Cr, which is adjacent to zinc and ranks as the fourth transition metal in terms of crustal abundance, is notable for its substantial natural reserves. This abundance facilitates its potential for large-scale, cost-effective commercial deployment. Cr exhibits remarkable stability in aqueous solutions. In its lower oxidation state of +3, it is capable of undergoing a three-electron transfer electrochemical reaction. As a negative electrode in metal anodes, this property endows chromium with a theoretical mass capacity of 1546 mAh g^{-1} and a theoretical volume capacity of 11118 mAh cm^{-3}, attributable to its three-electron lepton deposition/dissolution mechanism and its ideal density attributes. Moreover, with a standard reduction potential of −0.74 V, chromium is a promising candidate for the

expansion of the repertoire of high-performance HSCs, given its substantial theoretical capacity and favorable redox potential.

Building upon these intrinsic properties, researchers have initiated investigations into the potential use of chromium metal anodes in the field of energy storage. Recently, Sun and colleagues have successfully constructed a one-step-assembled chromium-ion hybrid supercapacitor (CHSC) by depositing metal Cr in the electrolyte on a PGCF substrate using high-performance porous graphitized carbon fabric (PGCF) as both the electrode collector and the anode active material (Figure 8a).[27] This represents the inaugural successful construction of a high-performance CHSC device. The researchers observed that Cr metal exhibited favorable deposition growth on the PGCF surface when a pre-deposition time of 30 min was employed, and the deposited layer consisting of denser irregular particles stored on the PGCF surface could be observed in high-resolution SEM images (Figure 8b avd c). As a result, at room temperature, as shown in Figure 8d avd e, the device demonstrated remarkable cycling stability, retaining 85.1% of its initial capacity after 300 cycles at 2 mA cm^{-2}, and only losing 4.6% of its initial capacity after 30000 cycles at 20 mA cm^{-2}, which provided excellent cycling stability. Figure 8f avd g demonstrate that the capacitance contribution in the CHSC device increases steadily with the scan rate and reaches 85% at 5 mV s^{-1}, which is one of the reasons why the CHSC exhibits excellent multiplicity characteristics. Based on the comparison of Ragone plots in Figure 8h, it can be found that the assembled CHSC can provide a maximum discharge power density of 9.95 mW cm^{-2} and a surface energy density of up to 1.47 mWh cm^{-2}, which is superior to most of the current aqueous HSCs in terms of charge storage energy. In addition, Sun et al. conducted further investigations into the electrochemical performance of CHSC at low temperatures. The electrochemical performance of CHSC at sustained temperature change in a discharge capacity and cycling stability test at −40 °C (Figure 8i avd j) showed the excellent low-temperature stability performance of CHSC, which is capable of maintaining a constant low-temperature capacity output. Furthermore, the capacity retention rate was observed to be as high as 99.5% after 8000 cycles. In Sun's study, a new type of CHSC was proposed and the potential application value of Cr anodes in AHSCs was confirmed. This finding provides a new idea for the design of low-temperature energy storage technology and indicates a new direction for the development of AHSCs.

In the research field of multivalent metal-ion HSCs, Cr anodes have attracted attention due to their high theoretical capacity and appropriate redox potential. Nevertheless, relatively few studies have been conducted on Cr metal anodes, and their high-capacity performance has not been fully explored and needs further research.

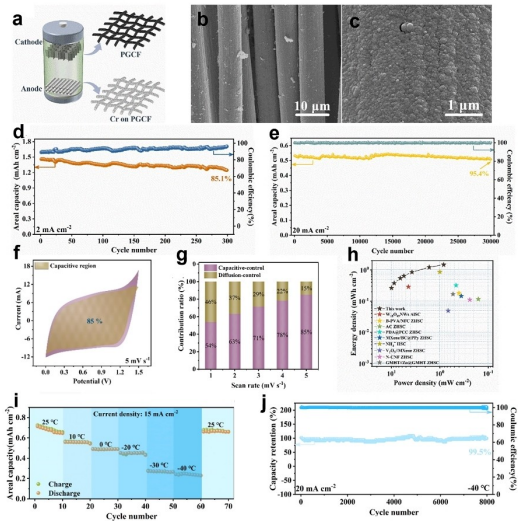

Figure 8. a) The assembly diagram of CHSC;[27] b,c) The characterization results of Cr anode: SEM images at different magnifications;[27] d) Cycle performance of CHSC-30 at 2 mA cm^{-2};[27] e) Cycle performance of CHSC-30 at 20 mA cm^{-2};[27] f) Capacitive contribution region of CHSC at 5 mV s^{-1};[27] g) The capacitive contribution ratios at different scan rates;[27] h) Ragone plot;[27] i) Charge capacities and discharge capacities of CHSC from 25 °C to −40 °C;[27] j) Cycle performance of CHSC at −40 °C.[27]

4.4. Others

Other multivalent metallic materials have also been reported as electrode materials for AHSCs, including but not limited to Fe_2O_3, cobalt (II) nitrate hexahydrate, $Ni(OH)_2$, and CuO.[87–90] Although iron oxide (FeO_x) has a wide working potential window and rich redox chemistry as an electrode material,[91,92] it also suffers from low specific capacitance and poor stability due to inherent drawbacks such as poor electronic conductivity and an insufficient ion diffusion rate.[93] Consequently, composite structures are often modulated to improve their electrochemical properties. For example, Wang et al.[94] report a novel Fe_2O_3 NTs@PPy/CC composite, synthesized using template and electrodeposition methods. SEM imaging (depicted in Figure 9a) confirms a conformable PPy coating on Fe_2O_3 nanotubes. The composite exhibits enhanced pseudocapacitive properties and stability. When combined with MnO_2 electrodes, the AHSC operates up to 2.0 V, delivering 59.4 μWh cm^{-2} areal energy density and 408.2 W kg^{-1} power density, as illustrated in Figure 9b. The device shows 92% capacitance retention and 100% coulombic efficiency over 6000 cycles at 40 mA cm^{-2}(Figure 9c). Combining iron oxide with other functional materials, such as conductive polymers, carbon nanotubes, or graphene, not only improves electronic conductivity, but also accelerates ionic transport, thereby increasing the rate capability and cycling capacity of the electrode material.

Cobalt-based electrode materials are renowned for their elevated specific capacitance and commendable electrical conductivity and have garnered extensive applications within the field of energy storage.[95] Liu's team[96] synthesized 2D MOF nanosheets, Co-BTB-LB, using a liquid-liquid interfacial method. HRTEM (Figure 9d avd e) shows the nanosheets' layered structure with organized nanopores, enhancing their activity for HSCs. The resulting AHSC with Co-BTB-LB and AC electrodes in KOH electrolyte achieved 150.2 Wh kg^{-1} energy density and 1619.2 W kg^{-1} power density, outperforming other materials-(Figure 9f). The device maintained 98% capacitance after 5000 cycles at 10 A g^{-1}(Figure 9g). Among the various forms of

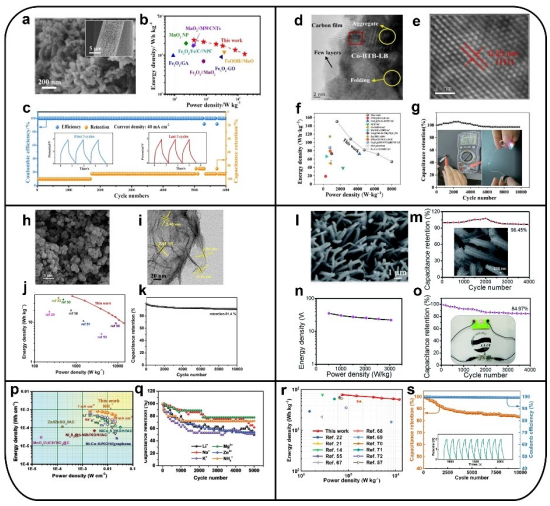

Figure 9. a) SEM images of Fe_2O_3 NTs@PPy/CC;[94] b) Ragone plot of AHSC assembled with this material vs. other high performance AHSCs;[94] c) Cycling performance at 40 mA cm^{-2} for 6000 cycles;[94] d) HRTEM image of Co-BTB-LB;[96] e) T Lattice spacing of the white structure in (d);[96] f) Ragone plot with other reported AHSCs materials;[96] g) Cycling stability test at the current density of 10 A g^{-1};[96] h) The SEM images of HMCS@Ni(OH)$_2$;[101] i) The HRTEM image of HMCS@Ni(OH)$_2$;[101] j) Ragone plots of the hybrid supercapacitor device;[101] k) Cycle performance of the hybrid supercapacitor device at a current density of 10 A g^{-1};[101] l) The SEM images of CVO Cu@CuO arrays;[104] m) Cycling performance of CVO Cu@CuO electrodes at 20 mA cm^{-2} current density;[104] n) A Ragone plot of the ASC;[104] o) Cycling performance at 4000 cycles at 3 A g^{-1} current;[104] p) Ragone plots of the MnO_2//ACC HSCs with different electrolytes;[108] q) Cycling performance of MnO_2//ACC HSCs;[108] r) Ragone plot of $CuCo_2S_4$@CP//AC AASC and recently reported AASCs;[109] s) Cycling performance of $CuCo_2S_4$@CP//AC AASC device at 10 A g^{-1}.[109]

cobalt-based electrode materials, those that fall within the category of MOFs have demonstrated particularly impressive performance characteristics, which can be attributed to three main factors: their high surface area, tunable pore size, and the presence of active cobalt sites. The integration of these characteristics confers a distinctive advantage on cobalt-based MOFs with regard to charge storage and release kinetics, thereby establishing them as a promising class of materials for next-generation energy storage systems.

Nickel-based materials such as nickel hydroxide, nickel oxide and nickel sulfide have been used as the electrode materials of SCs.[97–99] Specifically, $Ni(OH)_2$ has been identified as a key battery-type material, widely recognized for its high theoretical capacitance. However, the material presents certain challenges. It is prone to structural instability during the rapid processes of charge and discharge, which can impede its electrochemical performance.[100] To address this issue, researchers have endeavored to enhance the electrochemical attributes of $Ni(OH)_2$ through the incorporation of supplementary materials. Fu et al.[101] developed a hierarchical core-shell HMCS@Ni $(OH)_2$ nanocomposite via a bottom-up approach. The ultra-thin Ni $(OH)_2$ nanosheets on HMCS (Figure 9h avd i) provide a high surface area and improved conductivity. The AHSC using HMCS@Ni $(OH)_2$//HMCS electrodes achieves 45.84 Wh kg^{-1} energy density and 799 W kg^{-1} power density as illustrated in Figure 9j. The device maintains 91.4% capacitance after 10,000 cycles shown in Figure 9k. Notably, the addition of conductive carbon-based materials has emerged as a strategic approach.[102]

New progress is being made in the research of electrode materials for copper-based SCs. Copper-based materials, in particular CuO, have attracted interest as potential energy storage devices due to their distinctive electronic, mechanical and structural characteristics.[103] Liu's team[104] synthesized CVO CuO nanorod arrays on Cu foams via a simple in-situ oxidation method, as depicted in Figure 9l. The process creates slender nanosheets enveloping the nanorods, enhancing electrochemical activity. The CVO Cu@CuO electrode shows 96.45% capacitance retention after 4000 cycles (Figure 9m). The AHSC device, CVO Cu@CuO//AC, achieves 35.43 Wh kg^{-1} energy density and 520.99 W kg^{-1} power density, as portrayed in Figure 9ν, maintaining 84.97% capacitance after 4000 cycles, as shown in Figure 9o. However, despite the extensive research effort devoted to optimizing the morphology of copper oxide, challenges remain. Specifically, CuO-based materials are characterized by a relatively low specific capacitance, suboptimal energy density, and limited rate capability. These constraints can impede the overall performance of SCs, particularly in high-rate charge/discharge applications. To address these issues, it is essential to investigate innovative strategies for enhancing the electrochemical properties of Cu-based materials.

In addition, aqueous ammonia hybrid supercapacitors (AAHSCs), as an emerging electrode material, have attracted extensive attention from researchers.[105] These capacitors use ammonium ions (NH_4^+) as the electrolyte, which has a high operating voltage and is environmentally friendly. In aqueous ammonium root ion hybrid supercapacitors, the choice of electrode materials is also crucial. For instance, combining aqueous ammonium radical ions with conventional metal electrode materials has been shown to enhance the electrochemical performance of the electrode materials.[106,107] Chen and other researchers have successfully developed advanced layered δ-MnO_2-based HSCs.[108] The capacitor device employed layered δ-MnO_2 as the cathode material, activated carbon cloth as the anode material, and hydrated ammonium sulfate ($(NH_4)_2SO_4$) as the electrolyte. The device exhibits excellent electrochemical performance, reaching 861.2 μWh cm^{-2} in peak surface energy density (Figure 9p), and the capacitance retention is still as high as 72.2% after 5,000 charge/discharge cycles, as shown in Figure 9q, which significantly outperforms that of conventional metal-ion hybrid supercapacitors. Concurrently, Wu and his team successfully synthesized a high-performance electrode material ($CuCo_2S_4$@CP) with pseudocapacitive properties and applied it to AAHSCs initially.[109] When the $CuCo_2S_4$@CP electrode was combined with an activated carbon anode, the resulting $CuCo_2S_4$@CP//AC device exhibited a high cycling stability of 83.28% at a current density of 10 A g^{-1} and a high energy density of 74.17 Wh kg^{-1} (Figure 9r avd s), while exhibiting excellent device uniformity. In conclusion, the study of aqueous ammonium ion hybrid supercapacitors provides new ideas for the design and application of electrode materials and is expected to promote the further development of supercapacitors in the field of energy storage.

5. Conclusion and Prospects

In the development of new energy storage devices, two types of electrodes, namely capacitive and battery, are combined to pair HSCs that combine the respective advantages of batteries and SCs. In light of considerations of production cost, safety, and efficiency, an increasing number of research initiatives are now focusing their attention on transition-metal multivalent ionic AHSCs. These HSCs permit the utilization of less active metals as electrode material, while the employment of highly ionic conductive aqueous electrolytes can mitigate potential safety issues and increase power output. This review presents a brief overview of the energy storage mechanism of SCs and the structural features of AHSCs. It also reviews the selection of multivalent metal elements in AHSCs and provides a summary of some examples of AHSCs assembled with the participation of multivalent metals, based on the metal activity series. In recent years, significant advancements have been made in the research of AHSCs containing multivalent metals, which demonstrate considerable potential for the development of large-scale energy storage systems. Nevertheless, the field of research is still in its infancy and many issues require further investigation. Among the challenges facing ZHSCs are the formation of Zn dendrites and the generation of reaction by-products. These issues require breakthroughs in subsequent research, including electrode design, solutions for by-products, and device processing technologies. Concerning Mn-based aqueous hybrid energy storage devices, the HER reaction occurs at the Mn reduction deposition potential, resulting in a highly reversible deposition/stripping process of the Mn negative electrode that has not been fully realized in the current study. Further studies could begin with an investigation of the HER side reaction to achieve the high specific capacity characteristics of Mn. Among the metastable metals, the novel negative electrode of Cr is of particular interest. Although Cr has high theoretical mass and volumetric capacity, there has been a paucity of research conducted on Cr in AHSCs, and its high-capacity characteristics have not been fully exploited. Subsequently, other anode materials with excellent and stable energy storage characteristics can be selected to match with the Cr anode, thus obtaining energy storage devices with excellent performance. Furthermore, in aqueous environments, Fe, Co, Ni and Cu are not sufficiently stable and are prone to side reactions. Consequently, there is a paucity of single-metal materials that can be used as electrode materials in energy storage devices in AHSCs. Conversely, composite electrode materials are frequently constituted by the amalgamation of disparate metals or metal oxides. This approach facilitates the utilization of each material's distinct advantages, thereby compensating for the limitations inherent in employing a solitary material.

In order to increase the power density without sacrificing energy density and to achieve a balance between power and energy, future research needs to further explore AHSCs containing transition metals to enhance their conductivity and electrochemical stability by doping them with carbon materials, conductive polymers, etc., or by employing strategies such as elemental doping and introduction of defects. The employment of novel electrode structures, such as porous materials and nanostructures, is poised to enhance the number of active sites and optimize charge transfer efficiency. In tandem with this, the investigation of compatible electrolytes is set to expand the operating voltage window and improve electrochemical performance. The amalgamation of these research avenues with the development of novel corrosion-resistant electrode materials, surface modification technologies, wide voltage window electrolytes, optimized electrode-electrolyte interfaces, novel diaphragm materials and modular energy storage system designs, as well as the application of multifunctional electrode materials, flexible SCs, sustainable electrode materials, nanocapacitors, smart capacitors and 3D printing technologies is set to propel the AHSCs in the field of energy storage. This progression is poised to yield innovative solutions that promise to enhance the efficiency, safety and environmental sustainability of energy storage technologies.

Acknowledgements

We acknowledge the funding support by the National Natural Science Foundation of China (Grant No. 51902041). This theoretical calculation was carried out in part using computing resources at The National Supercomputing Center of Shenzhen.

Conflict of Interests

The authors declare that they have no known competing financial interests or personal relationships that could have appeared to influence the work reported in this paper.

Keywords: Aqueous hybrid supercapacitors · Electrode materials · Energy storage mechanisms · Multivalent metal elements · Transition metals

[1] Y. Gao, H. Zhang, X. Liu, Z. Yang, X. He, L. Li, Y. Qiao, S. Chou, *Adv. Energy Mater.* **2021**, *11*, 2101751.
[2] K. Alitabar, A. M. Zardkhoshoui, S. S. Hosseiny Davarani, *Batteries Supercaps* **2020**, *3*, 1311–1320.
[3] W. Lu, Y. Si, C. Zhao, T. Chen, C. Li, C. Zhang, K. Wang, *Chem. Eng. J.* **2024**, *495*, 153311.
[4] L. He, N. Wang, L. Sun, M. Xiang, L. Zhong, S. Komarneni, W. Hu, *Chem. Eng. J.* **2024**, *500*, 157271.
[5] Z. Pan, X. Liu, J. Yang, X. Li, Z. Liu, X. J. Loh, J. Wang, *Adv. Energy Mater.* **2021**, *11*, 2100608.
[6] J. B. Goodenough, *Energy Environ. Sci.* **2014**, *7*, 14–18.
[7] M. Wang, X. Zheng, X. Zhang, D. Chao, S. Qiao, H. N. Alshareef, Y. Cui, W. Chen, *Adv. Energy Mater.* **2021**, *11*, 2002904.
[8] D. He, J. Wang, Y. Peng, B. Li, C. Feng, L. Shen, S. Ma, *Sustain. Mater. Techno.* **2024**, *41*, e01017.
[9] M. He, S. Liu, J. Wu, J. Zhu, *Prog. Solid State Ch.* **2024**, *74*, 100452.
[10] F. Liu, Y. Zhang, H. Liu, S. Zhang, J. Yang, Z. Li, Y. Huang, Y. Ren, *ACS Nano* **2024**, *18*, 16063–16090.
[11] L. Liu, J. Zhang, Y. Zhao, M. Zhang, L. Wu, P. Yang, Z. Liu, *Chem. Commun.* **2024**, *60*, 1965–1978.
[12] Y. Wang, X. Wu, Y. Han, T. Li, *J. Energy Storage* **2021**, *42*, 103053.
[13] Y. Zhang, Q. Ma, S. Wang, X. Liu, L. Li, *ACS Nano* **2018**, *12*, 4824–4834.
[14] K. T. Selvi, K. A. Mangai, J. A. Lett, I. Fatimah, S. Sagadevan, *J. Energy Storage* **2024**, *92*, 112208.

[15] Y. Wang, B. Liu, Q. Li, S. Cartmell, S. Ferrara, Z. D. Deng, J. Xiao, *J. Power Sources* **2015**, *286*, 330–345.
[16] M. Xiang, J. Liao, N. Wang, L. Sun, L. He, X. Xie, S. Komarneni, G. Imanova, W. Hu, *Chem. Eng. J.* **2024**, *501*, 157620.
[17] Y. Shao, M. F. El-Kady, J. Sun, Y. Li, Q. Zhang, M. Zhu, H. Wang, B. Dunn, R. B. Kaner, *Chem. Rev.* **2018**, *118*, 9233–9280.
[18] S. Sheikh, A. Haghpanah Jahromi, *Monatsh. Chem.* **2024**, *155*, 383–399.
[19] M. Karlsmo, P. Johansson, *Batteries Supercaps* **2022**, *5*, e202200306.
[20] J. Fu, H. Wang, Z. Du, Y. Liu, Q. Sun, H. Li, *SmartMat* **2023**, *4*, e1182.
[21] X. Gong, J. Chen, P. S. Lee, *Batteries Supercaps* **2021**, *4*, 1529–1546.
[22] K. Zhang, Q. Zong, K. Ding, Y. Wang, L. Gao, D. Xu, Z. Chen, H. Yu, *Chem. Eng. J.* **2024**, *490*, 151369.
[23] L. Dong, W. Yang, W. Yang, Y. Li, W. Wu, G. Wang, *J. Mater. Chem. A* **2019**, *7*, 13810–13832.
[24] H. Wang, W. Ye, Y. Yang, Y. Zhong, Y. Hu, *Nano Energy* **2021**, *85*, 105942.
[25] B. Sun, N. Wang, X. Xie, L. Zhong, L. He, S. Komarneni, W. Hu, *J. Mater. Sci. Technol.* **2024**, *209*, 251–261.
[26] B. Sun, Y. Chen, N. Wang, Y. Wang, X. Xie, L. Zhong, L. He, S. Komarneni, W. Hu, *Small Struct.* **2023**, *4*, 2300077.
[27] < jnl >B. Sun, N. Wang, X. Xie, L. Zhong, L. He, M. Xiang, K. Liang, W. Hu, *Angew. Chem. Int. Ed.* **2024**, 63, e202408569(1 of 11)
[28] J. Zhu, T. Huang, M. Lu, X. Qiu, W. Zhang, *Green Chem.* **2024**, *26*, 5441–5451.
[29] W. Liu, H. Li, R. Y. Tay, *Nanoscale* **2024**, *16*, 4542–4562.
[30] H. Liu, X. Liu, S. Wang, H.-K. Liu, L. Li, *Energy Storage Mater.* **2020**, *28*, 122–145.
[31] Q. Gui, D. Ba, L. Li, W. Liu, Y. Li, J. Liu, *Sci. China Mater.* **2022**, *65*, 10–31.
[32] S. Rudra, H. W. Seo, S. Sarker, D. M. Kim, *Molecules* **2024**, *29*, 243.
[33] F. Béguin, V. Presser, A. Balducci, E. Frackowiak, *Adv. Mater.* **2014**, *26*, 2219–2251.
[34] J. Jiang, Y. Zhang, P. Nie, G. Xu, M. Shi, J. Wang, Y. Wu, R. Fu, H. Dou, X. Zhang, *Adv. Sustain. Syst.* **2018**, *2*, 1700110.
[35] A. A. Mohamad, *Inorg. Chem. Commun.* **2025**, *172*, 113677.
[36] Z. Tang, C. Tang, H. Gong, *Adv. Funct. Mater.* **2012**, *22*, 1272–1278.
[37] M. Xiang, N. Wang, L. Sun, L. He, L. Zhong, G. Imanova, S. Komarneni, W. Hu, *Sep. Purif. Technol.* **2025**, *354*, 128667.
[38] M. P. Down, S. J. Rowley-Neale, G. C. Smith, C. E. Banks, *ACS Appl. Energy Mater.* **2018**, *1*, 707–714.
[39] C. Liu, Z. Yu, D. Neff, A. Zhamu, B. Z. Jang, *Nano Lett.* **2010**, *10*, 4863–4868.
[40] K. H. An, W. S. Kim, Y. S. Park, Y. C. Choi, S. M. Lee, D. C. Chung, D. J. Bae, S. C. Lim, Y. H. Lee, *Adv. Mater.* **2001**, *13*, 497–500.
[41] G.-R. Li, Z.-P. Feng, Y.-N. Ou, D. Wu, R. Fu, Y.-X. Tong, *Langmuir* **2010**, *26*, 2209–2213.
[42] J. M. Miller, B. Dunn, T. D. Tran, R. W. Pekala, *J. Electrochem. Soc.* **1997**, *144*, L309–L311.
[43] Y. Shao, M. F. El-Kady, J. Sun, Y. Li, Q. Zhang, M. Zhu, H. Wang, B. Dunn, R. B. Kaner, *Chem. Rev.* **2018**, *118*, 9233–9280.
[44] V. Augustyn, P. Simon, B. Dunn, *Energy Environ. Sci.* **2014**, *7*, 1597.
[45] P. Tang, W. Tan, G. Deng, Y. Zhang, S. Xu, Q. Wang, G. Li, J. Zhu, Q. Dou, X. Yan, *Energy Environ. Mater.* **2023**, *6*, e12619.
[46] C. Xu, J. Mu, T. Zhou, S. Tian, P. Gao, G. Yin, J. Zhou, F. Li, *Adv. Funct. Mater.* **2022**, *32*, 2206501.
[47] J. Liu, J. Wang, C. Xu, H. Jiang, C. Li, L. Zhang, J. Lin, Z. X. Shen, *Adv. Sci.* **2018**, *5*, 1700322.
[48] J. Wang, S. Dong, B. Ding, Y. Wang, X. Hao, H. Dou, Y. Xia, X. Zhang, *Natl. Sci. Rev.* **2017**, *4*, 71–90.
[49] X. Wang, Y. Wang, J. Hao, Y. Liu, H. Xiao, Y. Ma, L. Chen, Y. Huang, G. Yuan, *Energy Storage Mater.* **2022**, *50*, 454–463.
[50] J. B. Cook, T. C. Lin, H.-S. Kim, A. Siordia, B. S. Dunn, S. H. Tolbert, *ACS Nano* **2019**, *13*, 1223–1231.
[51] R. Zhang, X. Yang, S. Xu, D. Xu, F. Du, *Phys. Chem. Chem. Phys.* **2019**, *21*, 25940–25944.
[52] A. K. Tomar, T. Kshetri, N. H. Kim, J. H. Lee, *Energy Storage Mater.* **2022**, *50*, 86–95.
[53] J. Libich, J. Máca, J. Vondrák, O. Čech, M. Sedlaříková, *J. Energy Storage* **2018**, *17*, 224–227.
[54] G. G. Amatucci, F. Badway, A. Du Pasquier, T. Zheng, *J. Electrochem. Soc.* **2001**, *148*, A930.
[55] G. G. Bizuneh, A. M. M. Adam, J. Ma, *Battery Energy* **2023**, *2*, 20220021.
[56] M. Czagany, S. Hompoth, A. K. Keshri, N. Pandit, I. Galambos, Z. Gacsi, P. Baumli, *Materials (Basel)* **2024**, *17*, 702.
[57] M. N. Sakib, S. Ahmed, S. M. S. M. Rahat, S. B. Shuchi, *J. Storage* **2021**, *44*, 103322.
[58] S. Sahani, H. Mahajan, S. S. Han, *J. Energy Storage* **2024**, *90*, 111808.
[59] A. C. Forse, J. M. Griffin, C. Merlet, J. Carretero-Gonzalez, A.-R. O. Raji, N. M. Trease, C. P. Grey, *Nat. Energy* **2017**, *2*, 16216.
[60] Z. Bo, M. Zhou, S. Zhou, Y. Song, Z. Liu, H. Liao, H. Yang, J. Yan, K. Cen, X. Fan, Q. Yu, K. (Ken) Ostrikov, J. Li, *Adv. Funct. Mater.* **2022**, *32*, 2207140.
[61] J. Lu, J. Zhang, X. Wang, J. Zhang, Z. Tian, E. Zhu, L. Yang, X. Guan, H. Ren, J. Wu, X. Li, G. Wang, *J. Energy Storage* **2024**, *103*, 114338.
[62] S. Park, Y. Lee, G. An, *Int J Energy Res.* **2021**, *45*, 16027–16037.
[63] L. Yu, G. Z. Chen, *Front. Chem.* **2019**, *7*, 272.
[64] S. Bi, R. Wang, S. Liu, J. Yan, B. Mao, A. A. Kornyshev, G. Feng, *Nat. Commun.* **2018**, *9*, 5222.
[65] X. Wang, H. Zhou, E. Sheridan, J. C. Walmsley, D. Ren, D. Chen, *Energy Environ. Sci.* **2016**, *9*, 232–239.
[66] M. Galiński, A. Lewandowski, I. Stępniak, *Electrochim. Acta* **2006**, *51*, 5567–5580.
[67] G. Liang, F. Mo, X. Ji, C. Zhi, *Nat. Rev. Mater.* **2020**, *6*, 109–123.
[68] D. P. Dubal, O. Ayyad, V. Ruiz, P. Gómez-Romero, *Chem. Soc. Rev.* **2015**, *44*, 1777–1790.
[69] A. Muzaffar, M. B. Ahamed, K. Deshmukh, J. Thirumalai, *Renew. Sust. Energ. Rev.* **2019**, *101*, 123–145.
[70] M. Kandasamy, S. Sahoo, S. K. Nayak, B. Chakraborty, C. S. Rout, *J. Mater. Chem. A* **2021**, *9*, 17643–17700.
[71] S. Jha, S. Mehta, Y. Chen, R. Likhari, W. Stewart, D. Parkinson, H. Liang, *Energy Storage* **2020**, *2*, e184.
[72] M. K. Devaraju, I. Honma, *Adv. Energy Mater.* **2012**, *2*, 284–297.
[73] N. S. Arul, J. I. Han, D. Mangalaraj, *J. Mater. Sci: Mater. Electron.* **2018**, *29*, 1636–1642.
[74] Q. Qu, P. Zhang, B. Wang, Y. Chen, S. Tian, Y. Wu, R. Holze, *J. Phys. Chem. C* **2009**, *113*, 14020–14027.
[75] T. Gu, B. Wei, *J. Mater. Chem. A* **2016**, *4*, 12289–12295.
[76] Z. Wu, X. Zhang, X. Jin, T. Li, J. Ge, Z. Li, *J. Nanomater.* **2021**, *2021*, 1–17.
[77] B. Liu, Y. Sun, L. Liu, S. Xu, X. Yan, *Adv. Funct. Mater.* **2018**, *28*, 1704973.
[78] A. Emin, J. Li, Y. Dong, Y. Fu, D. He, Y. Li, *J. Storage Mater.* **2023**, *65*, 107340.
[79] S. Zhang, L. Li, Y. Liu, Q. Li, *Carbohyd. Polym.* **2024**, *326*, 121661.
[80] X. Li, Z. Lin, C. Wang, H. Wang, S. Feng, T. Li, Y. Ma, *Chem. Eng. J.* **2024**, *484*, 149430.
[81] Y. Liu, Z. Zeng, B. Bloom, D. H. Waldeck, J. Wei, *Small* **2018**, *14*, 1703237.
[82] Y. Shen, Y. Liu, K. Sun, T. Gu, G. Wang, Y. Yang, J. Pang, Y. Zheng, X. Yang, L. Chen, *J. Mater. Sci. Technol.* **2024**, *169*, 137–147.
[83] C. Wang, X. Zeng, P. J. Cullen, Z. Pei, *J. Mater. Chem. A* **2021**, *9*, 19054–19082.
[84] F. Wei, H. Zhang, X. Hui, Y. Lv, S. Ran, X. Liu, *J. Power Sources* **2023**, *554*, 232348.
[85] X. Li, Y. Li, S. Xie, Y. Zhou, J. Rong, L. Dong, *Chem. Eng. J.* **2022**, *427*, 131799.
[86] J. Huo, X. Wang, X. Zhang, L. Zhang, G. Yue, S. Guo, *J. Energy Storage* **2023**, *73*, 108925.
[87] Y. Wang, Z. Du, J. Xiao, W. Cen, S. Yuan, *Electrochim. Acta* **2021**, *386*, 138486.
[88] Q. Liu, Z. Guo, C. Wang, S. Guo, Z. Xu, C. Hu, Y. Liu, Y. Wang, J. He, W. Wong, *Adv. Sci.* **2023**, *10*, 2207545.
[89] Y. Fu, Y. Zhou, Q. Peng, C. Yu, Z. Wu, J. Sun, J. Zhu, X. Wang, *J. Power Sources* **2018**, *402*, 43–52.
[90] Y. Liu, X. Cao, D. Jiang, D. Jia, J. Liu, *J. Mater. Chem. A* **2018**, *6*, 10474–10483.
[91] W. Raza, F. Ali, N. Raza, Y. Luo, K.-H. Kim, J. Yang, S. Kumar, A. Mehmood, E. E. Kwon, *Nano Energy* **2018**, *52*, 441–473.
[92] X. Zhang, N. Peng, T. Liu, R. Zheng, M. Xia, H. Yu, S. Chen, M. Shui, J. Shu, *Nano Energy* **2019**, *65*, 104049.
[93] H. Yang, S. Kannappan, A. S. Pandian, J.-H. Jang, Y. S. Lee, W. Lu, *Nanotechnology* **2017**, *28*, 445401.
[94] Y. Wang, Z. Du, J. Xiao, W. Cen, S. Yuan, *Electrochim. Acta* **2021**, *386*, 138486.
[95] L. Yang, Q. Zhu, K. Yang, X. Xu, J. Huang, H. Chen, H. Wang, *Nanomaterials (Basel)* **2022**, *12*, 4065.
[96] Q. Liu, Z. Guo, C. Wang, S. Guo, Z. Xu, C. Hu, Y. Liu, Y. Wang, J. He, W. Wong, *Adv. Sci.* **2023**, *10*, 2207545.
[97] L. Hu, L. Wu, M. Liao, X. Hu, X. Fang, *Adv. Funct. Mater.* **2012**, *22*, 998–1004.
[98] L. Ma, R. Liu, L. Liu, F. Wang, H. Niu, Y. Huang, *J. Power Sources* **2016**, *335*, 76–83.

[99] X. Wang, S.-X. Zhao, L. Dong, Q.-L. Lu, J. Zhu, C.-W. Nan, *Energy Storage Mater.* **2017**, *6*, 180–187.
[100] S.-I. Kim, S.-W. Kim, K. Jung, J.-B. Kim, J.-H. Jang, *Nano Energy* **2016**, *24*, 17–24.
[101] Y. Fu, Y. Zhou, Q. Peng, C. Yu, Z. Wu, J. Sun, J. Zhu, X. Wang, *J. Power Sources* **2018**, *402*, 43–52.
[102] W. Niu, Z. Xiao, S. Wang, S. Zhai, L. Qin, Z. Zhao, Q. An, *J. Alloy. Compd.* **2021**, *853*, 157123.
[103] D. Majumdar, S. Ghosh, *J. Energy Storage* **2021**, *34*, 101995.
[104] Y. Liu, X. Cao, D. Jiang, D. Jia, J. Liu, *J. Mater. Chem. A* **2018**, *6*, 10474–10483.
[105] J. Dai, Y. Yang, J. Yu, H. Fu, Y. Xu, Q. Qin, X. Qi, L. Dai, A. Cabot, *Chem. Eng. J.* **2024**, *500*, 157343.
[106] X.-L. Han, J. Zhang, Z.-S. Wang, H. A. Younus, D.-W. Wang, *Rare Met.* **2024**, *43*, 5734–5746.
[107] T. Xiao, C. Tang, H. Lin, X. Li, Y. Mei, C. Xu, L. Gao, L. Jiang, P. Xiang, S. Ni, Y. Xiao, X. Tan, *Inorg. Chem.* **2024**, *63*, 17714–17726.
[108] Q. Chen, J. Jin, M. Song, X. Zhang, H. Li, J. Zhang, G. Hou, Y. Tang, L. Mai, L. Zhou, *Adv. Mater.* **2022**, *34*, 2107992.
[109] Q. Wu, Y. Zhang, G. Liu, X. Cui, S. Tao, H. Jiang, Y. Lin, R. Peng, X. Zhang, Z. Huang, Y. Song, Y. Ding, S. M. Akhlaq, Y. Wu, K. Tao, E. Xie, Z. Zhang, Z.-S. Wu, *Energy Storage Mater.* **2024**, *70*, 103474.

Manuscript received: October 18, 2024
Revised manuscript received: January 3, 2025
Accepted manuscript online: January 19, 2025
Version of record online: February 17, 2025